Molecular Dynamics Simulation Study for Transport Properties of Diatomic Liquids

Song Hi Lee

Department of Chemistry, Kyungsung University, Busan 608-736, Korea. E-mail: shlee@ks.ac.kr

We present results for transport properties of diatomic fluids by isothermal-isobaric (NpT) equilibrium molecular dynamics (EMD) simulations using Green-Kubo and Einstein formulas. As the molecular elongation of diatomic molecules increases from the spherical monatomic molecule, the diffusion coefficient increases, indicating that longish shape molecules diffuse more than spherical molecules, and the rotational diffusion coefficients are almost the same in the statistical error since random rotation decreases. The calculated translational viscosity decreases with the molecular elongation of diatomic molecule within statistical error bar, while the rotational viscosity increases. The total thermal conductivity decreases as the molecular elongation increases. This result of thermal conductivity for diatomic molecules by EMD simulations is again inconsistent with the earlier results of those by non-equilibrium molecular dynamics (NEMD) simulations even though the missing terms related to rotational degree of freedom into the Green-Kubo and Einstein formulas with regard to the calculation of thermal conductivity for molecular fluids are included.

Key Words : Diffusion, Shear viscosity, Thermal conductivity, Diatomic liquids, Molecular dynamics simulation

Introduction

The earliest molecular dynamics (MD) calculations on polyatomic fluids have been carried out by Harp and Berne[1] using a Stockmayer-type potential to simulate CO and N_2 and by Rahman and Stillinger[2] to simulate H_2O. For dumbbell diatomic molecules, a very simple extension of the hard-sphere model is to consider a diatomic composed of two hard spheres fused together,[3] but more realistic models involve continuous potentials. Thus, N_2, F_2, Cl_2 *etc.* have been depicted as two 'Lennard-Jones atoms' separated by a fixed bond length.[4-6]

Lee and Cummings[7] reported results of non-equilibrium molecular dynamics (NEMD) simulations for shear viscosities of pure quadrupolar fluids, a pure dipolar quadrupolar fluid, non-quadrupolar/quadrupolar mixtures, and quadrupolar/quadrupolar mixtures. They found that the addition of quadrupolar interactions to the pure Ar and to the pure dipolar Ar leads to a higher viscosities as was observed in the addition of dipolar interaction to the pure Ar.[8] They continued to report results of NEMD simulations for shear viscosities of pure diatomic fluids, monatomic/diatomic mixtures, and diatomic/diatomic mixtures.[9] It was found that the interaction between diatomic molecules is less attractive than that between spherical molecules which leads to lower viscosities as was observed in the experimental fact that the viscosity of normal alkanes is less than that of branched alkanes.

Recently, Tokumasu *et al.*[10] have studied the effect of molecular elongation on the thermal conductivity of diatomic liquids using a NEMD method. It was found that the reduced thermal conductivity increases as molecular elongation increases. Detailed analysis of the molecular contribution to the thermal conductivity revealed that the contribution of the flux caused by energy transport and by translational energy transfer to the thermal conductivity is independent of the molecular elongation, and the contribution of the heat flux caused by rotational energy transfer to the thermal conductivity increases with the increase in the molecular elongation.

More recently, Vrabec *et al.*[11] calculated shear viscosity and thermal conductivity of ten fluids, modeled by the two-center Lennard-Jones plus point quadrupole (2CLJQ) pair potential, using equilibrium molecular dynamics simulation with the Green-Kubo formalism. They found that at low temperature and high density states, the Green-Kubo integral for shear viscosity shows slow convergence. This problem was overcome by a new approach which is based on the adjustment of a suitable function describing the long time behavior of the auto-correlation function and yields reliable results without the need of excessively long simulations runs.

In the present paper, we report equilibrium MD simulations for the systems of spherical monatomic and several dumbbell diatomic molecules. The primary study goal is to analyze the dependence of transport properties of diatomic molecules on molecular elongation. This paper is organized as follows : We present the molecular models and the technical details of MD simulation in the following section, some theoretical aspects in Section III, our results in Section IV, and concluding remarks in Section V.

Molecular Models and MD Simulation Methods

The diatomic molecule is modeled as the two-center Lennard-Jones potential.[6] The total interaction is a sum of pairwise contributions from distinct atoms a in molecule i, at position r_{ia}, and b in molecule j, at position r_{jb}:

$$u_{ij}(\mathbf{r}_{ij}) = \sum_{a=1}^{2} \sum_{b=1}^{2} u_{ab}(r_{ab}), \qquad (1)$$
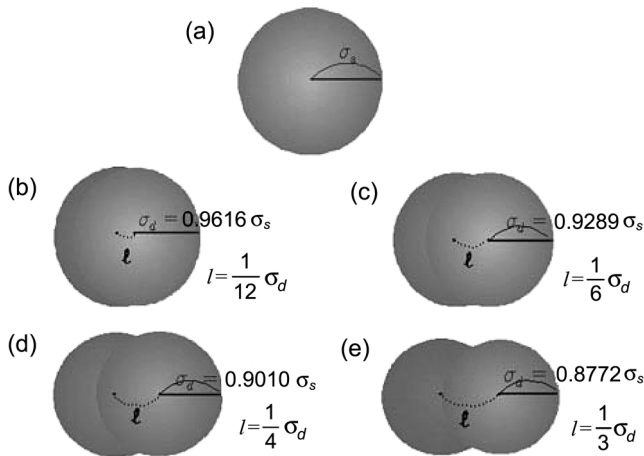
Figure 1. Monatomic and diatomic molecules.

where r_{ab} is the inter-site separation $r_{ab} = |r_{jb} - r_{jb}|$ and u_{ab} is the pair potential acting between sites a and b:

$$u_{ab}(r_{ab}) = 4\varepsilon_d \left[\left(\frac{\sigma_d}{r_{ab}} \right)^{12} - \left(\frac{\sigma_d}{r_{ab}} \right)^6 \right]. \qquad (2)$$

Here ε_d and σ_d are the Lennard-Jones (LJ) parameters for each site of the diatomic molecule. The interatomic separation in a diatomic molecule, l, is chosen such as the volume of the diatomic molecule is the same as that of a sphere of diameter σ_s. Since the volume of a diatomic molecule of two spheres of diameter s_d is given by

$$V_d = \frac{1}{6}\pi\sigma_d^3 + \frac{1}{4}\pi\sigma_d^2 l + \frac{1}{12}\pi l^3, \qquad (3)$$

for a given interatomic separation $l = L\sigma_d$, σ_d is determined by equating $V_d = V_s$, and can be expressed in the form of $\sigma_d = c\sigma_s$. In this study, we have chosen as L=0, 1/12, 1/6, 1/4, and 1/3, and the corresponding c is determined as 1.0, 0.9616, 0.9289, 0.9010, and 0.8772, respectively, as shown in Figure 1. The other LJ parameter ε_d is chosen as $\varepsilon_s/4$. The LJ parameters, σ_s and ε_s, for the spherical Ar are chosen as 0.3405 nm and 0.9961 kJ/mol, respectively.

All EMD simulations were carried on 1728 molecules in isothermal-isobaric (NpT fixed) ensemble and fully equilibrated for at least 500,000 time steps of 10^{-15} second (1 femto second). The equilibrium properties were then averaged over 5 blocks of 200,000 time steps for a total of 1,000,000 time steps (1 nano second), and the configurations of molecules were stored every 10 time steps for later analysis of structural and dynamic properties. The intermolecular potentials were subject to a spherical cutoff as follows: the cutoff distance was $2.5\sigma_s$ for pure diatomic fluids. The equations of translational motion in NpT ensemble were devised by a constraint method[12] and solved using a fifth-order, predictor-corrector, Gear integration,[13] and the equations of rotational motion about the center of mass for molecular fluids in NpT ensemble were derived using quaternions.[14-16]

Theorem

As dynamic properties, we consider diffusion constant (D), viscosity (η), and thermal conductivity (λ) of diatomic liquid systems.

Diffusion constant. Translational diffusion constant (D_t) can be obtained through two routes: the Green-Kubo formula from velocity auto-correlation functions (VAC) :

$$\Delta_\tau = \frac{1}{3}\int_0^\infty < v_i(t) \cdot v_i(0) > \mathrm{d}t \qquad (4)$$

and the Einstein formula from mean square displacements (MSD) :

$$D_t = \frac{1}{6}\lim_{t \to \infty} \frac{d < |r_i(t) - r_i(0)|^2 >}{\mathrm{d}t}. \qquad (5)$$

The contribution to diffusion by rotational motion of diatomic molecule is represented by rotational diffusion constant:

$$D_r = \frac{l^2}{2}\int_0^\infty < w_i(t) \cdot w_i(0) > \mathrm{d}t \qquad (6)$$

and

$$D_r = \frac{l^2}{4}\lim_{t \to \infty} \frac{d < |e_i(t) - e_i(0)|^2 >}{\mathrm{d}t}. \qquad (7)$$

Here $\mathbf{w}_i(t)$ and $\mathbf{e}_i(t)$ are the angular velocity and the unit orientation vector of diatomic molecule i, respectively. The denominators of 2 and 4 in Eqs. (6) and (7) are due to 2 degrees of freedom of rotational motion.

Shear viscosity. Shear viscosity by translational motion is calculated by a modified Green-Kubo formula for better statistical accuracy[17]:

$$\eta_t = \frac{V}{kT}\int_0^\infty \mathrm{d}t \sum_i < P_{i\alpha\beta}^t(0) \cdot P_{i\alpha\beta}^t(t) >, \qquad (8)$$

where $P_{i\alpha\beta}^t$ is the $\alpha\beta$ component of the molecular stress tensor, P_i^t, of particle i by translational motion :

$$P_{i\alpha\beta}^t(t) = \frac{1}{V}[mv_{i\alpha}(t)v_{i\beta}(t) + r_{i\alpha}(t)f_{i\beta}(t)]. \qquad (9)$$

There is another formula for $P_{i\alpha\beta}^t$:

$$P_{i\alpha\beta}^t(t) = \frac{1}{V}\left[mv_{i\alpha}(t)v_{i\beta}(t) + \sum_{j \neq i} r_{ij\alpha}(t)f_{ij\beta}(t)\right]. \qquad (10)$$

where $\alpha\beta$ = xy, xz, yx, yz, zx, or zy. The equality of Eqs. (9) and (10) with Σ_i is discussed in Ref..[18] It is recommended to use Eq. (10) in a simulation that employs periodic boundary condition.

Shear spin viscosity by rotational motion is calculated by a similar way to translational motion[19]:

$$\eta_r = \frac{V}{kT}\int_0^\infty \mathrm{d}t \sum_i < P_{i\alpha\beta}^r(0) \cdot P_{i\alpha\beta}^r(t) >, \qquad (11)$$

where two formulas for $P_{i\alpha\beta}^r$:

$$P^r_{i\alpha\beta}(t) = \frac{1}{V}[mv_{i\alpha}(t)Iw_{i\beta}(t) + r_{i\alpha}(t)N_{i\beta}(t)] \qquad (12)$$

and

$$P^r_{i\alpha\beta}(t) = \frac{1}{V}\left[mv_{i\alpha}(t)Iw_{i\beta}(t) + \sum_{j\neq i} r_{ij\alpha}(t)N_{ij\beta}(t)\right], (13)$$

where N_i denotes the torque on the molecules I.

Thermal conductivity. Thermal conductivity is calculated by a modified Green-Kubo formula for better statistical accuracy[17]:

$$\lambda = \frac{V}{kT^2}\int_0^\infty dt \sum_i <\dot{q}_{i\alpha}(0)\dot{q}_{i\alpha}(t)> , \qquad (14)$$

where $\alpha = x$, y, and z, and the total heat flux by molecule i is

$$\dot{q}_{i\alpha}(t) = \frac{1}{V}\left\{ \varepsilon_i(t)v_{i\alpha}(t) \right.$$
$$\left. + \frac{1}{2}\sum_{j\neq i} r_{ij\alpha}(t)[v_i(t)\cdot f_{ij}(t) + w_i^p(t)\cdot N_{ij}^p(t)] \right\}. \quad (15)$$

Here, the superscript p indicates the principle axis frame and the total energy of molecule i is given by

$$\varepsilon_i(t) = \frac{1}{2}m_i v_i(t)^2 + \frac{1}{2}Iw_i(t)^2 + \frac{1}{2}\sum_{j\neq i}\Phi[r_{ij}(t)]. \quad (16)$$

where $\Phi(r_{ij})$ denotes the potential energy between molecules i and j.

The heat flux by each molecule, Eq. (15), with the energy of molecule, Eq. (16), consists of five contributions :

$$\dot{q}_{i\alpha} = \dot{q}^{tt}_{i\alpha} + \dot{q}^{tr}_{i\alpha} + \dot{q}^{tp}_{i\alpha} + \dot{q}_{i\alpha}, \qquad (17)$$

and there are two different molecular mechanism responsible for heat flux in liquids, namely, energy transport due to molecular motion and energy transfer due to molecular interaction. These mechanisms correspond to the first and second terms on the right-hand side of Eq. (15), respectively, which are called the *transport term* and the *interaction term*. The heat flux caused by molecular motion consists of three contributions of translational, rotational and potential energy transport, which correspond to the first, second and third terms in Eq. (16), respectively. The contributions to the heat flux due to translational, rotational and potential energy transport are defined, respectively, by

$$\dot{q}^{tt}_{i\alpha} = \frac{1}{V}\left[\frac{1}{2}m_i v_i^2\right]v_{i\alpha}, \qquad (18)$$

$$\dot{q}^{tr}_{i\alpha} = \frac{1}{V}\left[\frac{1}{2}Iw_i^2\right]v_{i\alpha}, \qquad (19)$$

and

$$\dot{q}^{tp}_{i\alpha} = \frac{1}{V}\left[\frac{1}{2}\sum_{j\neq i}\Phi(r_{ij})\right]v_{i\alpha}. \qquad (20)$$

The heat flux caused by molecular interaction consists of two contributions of translational and rotational energy transfer, which corresponds to the first and second terms in

the interaction term in Eq. (15). The heat flux caused by translational and rotational energy transfer is defined by

$$\dot{q}^{it}_{i\alpha} = \frac{1}{V}\left[\sum_{j\neq i}\frac{1}{2}r_{ij\alpha}(v_i\cdot f_{ij})\right], \qquad (21)$$

and

$$\dot{q}^{ir}_{i\alpha} = \frac{1}{V}\left[\sum_{j\neq i}\frac{1}{2}r_{ij\alpha}(w_i^p\cdot N_{ij}^p)\right], \qquad (22)$$

respectively. Hence, the thermal conductivity, Eq. (14), consists of five contributions :

$$\lambda_{tot} = \lambda_{tt} + \lambda_{tr} + \lambda_{tp} + \lambda_{it} + \lambda_{ir}. \qquad (23)$$

Results and Discussion

NpT EMD simulations for monatomic and diatomic molecular systems carried out with a careful consideration of the long-range correction due to the spherical cut-off the potential, which is a tail correction estimating the contribution from pairs of particles whose distance apart is greater than the cut-off distance.[20,21] Thermodynamic properties for monatomic and diatomic molecules at 94.4 K in NpT ensemble obtained from our EMD simulations are listed in Table 1. The Lennard-Jones(LJ) energy and total energy decrease negatively with increasing interatomic separation in a diatomic. This means that the interaction between diatomic molecules becomes less attractive with the

Table 1. Lennard-Jones energy (E_{LJ} in kJ/mol), total energy (E_{tot} in kJ/mol), pressure (p in atm), volume (V in nm^3) and of diatomic molecules at 94.4 K in NpT ensembles. Uncertainties (standard deviations) in the last reported digit(s) are given in parenthesis.

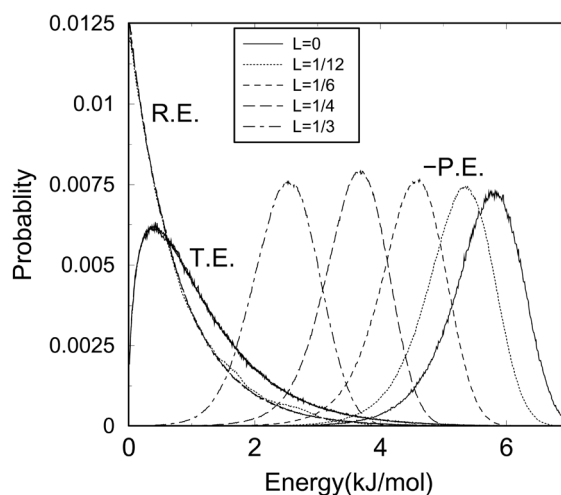| Properties	L = 0	L = 1/12	L = 1/6	L = 1/4	L = 1/3
-E_{LJ}	5.339(5)	5.196(8)	4.455(5)	3.555(9)	2.404(6)
-E_{tot}	4.161(5)	3.234(8)	2.493(5)	1.592(9)	0.502(6)
p	−0.407(3)	0.969(2)	1.03(2)	1.05(3)	1.09(4)
V	84.21(49)	78.81(44)	79.93(52)	88.01(24)	113.0(10)

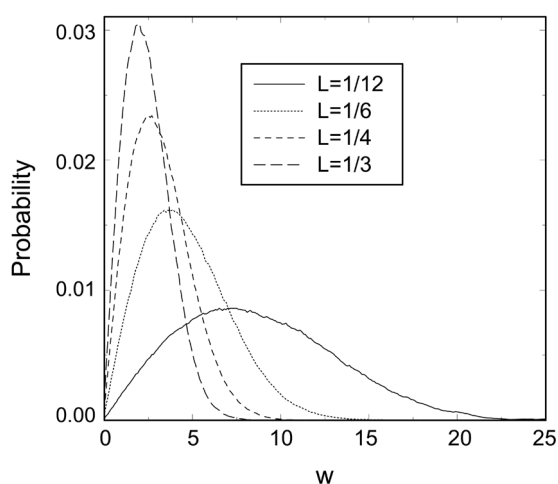
Figure 2. Energy distributions.
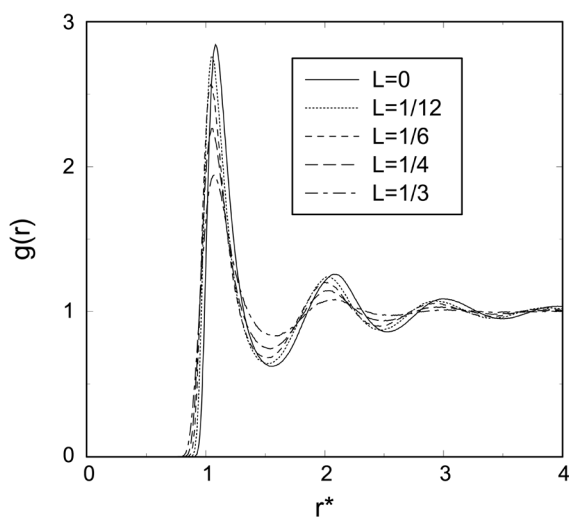
Figure 3. Angular speed distributions.

Figure 4. Radial distribution functions.

increase in the molecular elongation. The calculated pressures in NpT EMD simulations are much close to 1 atm except the monatomic molecular system. The modification from the sphere of diameter s_s to the diatomic system of L=1/12 brings a volume decrease from $84 \, nm^3$ to $79 \, nm^3$ and then the volume increases with the value of L. Also note that beyond the elongation of L=1/3, for example, in the diatomic molecular systems of L=5/12 and 1/2, the system becomes infinite dilution, keeping the pressure of the system as 1 atm.

Figure 2 shows the energy distributions of the potential energy (P.E.), translational kinetic energy (T.E.), and rotational kinetic energy (R.E.) of monatomic and diatomic molecules. The P.E. decreases negatively with increasing interatomic separation in a diatomic as seen in Table 1. The distribution of T.E. displays a typical Maxwell-Boltzman energy distribution $[f(\varepsilon) \sim \sqrt{\varepsilon} \ e^{-\varepsilon/kT}]$ while that of R.E. indicates a lot of diatomic molecules do not rotate at T = 94.4 K. However, this may lead a misunderstanding of rotational speed distribution, which is a typical Maxwell-

Boltzman energy distribution as shown in Figure 3.

Figure 4 shows the center-center radial distribution functions, g(r), of monatomic and diatomic molecules at 94.4 K in NpT ensemble. As the molecular elongation increases, the first and second peaks in the center of mass g(r) diminish gradually and the minima increase. It is also observed that the nearest distance between centers of diatomic molecules becomes shorter with the increase in the molecular elongation. This is because the centers of mass of diatomic molecules come closer as the molecular elongation increases.

Table 2 lists the translational and rotational diffusion coefficients of monatomic and diatomic molecules at 94.4 K obtained through the Green-Kubo and Einstein formulas. The velocity auto-correlation function and mean square displacement of monatomic and diatomic molecules are well-behaved (data not shown) as seen in the standard deviation for the translational diffusion coefficients. As the molecular elongation of diatomic molecule increases from the spherical monatomic molecule, the translational diffusion coefficient increases. This means that a rod-like molecule diffuses more than a spherical molecule as seen in *n*-butane and *i*-butane.

Employing two formals, Eqs. (6) and (7), to calculate the rotational diffusion coefficients, there exists two difficulties. First, in the Green-Kubo formula, Eq. (6), the angular velocity auto-correlation function for L=1/12 does not decay to zero in the long time as shown in Figure 5 and the resulting rotational diffusion coefficient goes infinity. This is because the interatomic separation is so short that the diatomic molecule persists not to rotate even though the torque is large. Second, in the Einstein formula, Eq. (7), the mean square displacements of unit orientation vector $e_i(t)$ are not a linear function of time as seen in Figure 6 because the value of $e_i(t)$ is unit. As a result, we were not able to calculate the rotational diffusion coefficients from Eq. (7). The value of the mean square displacements of unit orientation vector approaches to 2 as time goes infinity since in the following equation :

$$\lim_{t \to \infty} \langle |e_i(t) - e_i(0)|^2 \rangle$$

$$= \lim_{t \to \infty} [\langle |e_i(t)|^2 \rangle + \langle |e_i(0)|^2 \rangle - 2 \langle |e_i(t) \cdot e_i(0)|^2 \rangle]$$

$$= 2 - 2 \lim_{t \to \infty} \langle |e_i(t) \cdot e_i(0)| \rangle \qquad (24)$$

Table 2. Translational (D_t) and rotational diffusion coefficients (D_r, $10^{-5} \, cm^2/sec$) of monatomic and diatomic molecules at 94.4 K obtained through the Green-Kubo and Einstein formulas. Uncertainties (standard deviations) in the last reported digit(s) are given in parenthesis

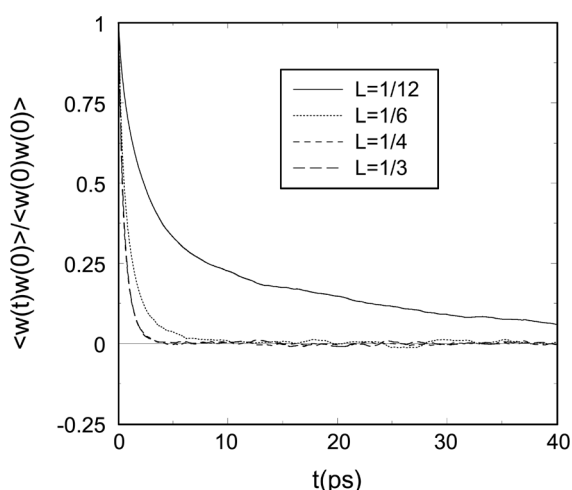| D	L = 0	L = 1/12	L = 1/6	L = 1/4	L = 1/3
D_t, Eq. (4)	2.55(4)	2.77(5)	3.65(13)	5.48(13)	9.93(83)
D_t, Eq. (5)	2.54(4)	2.92(7)	3.81(13)	5.24(11)	8.53(68)
D_r, Eq. (6)	–	–	136(9)	90.1(4)	90.8(14)

Figure 5. Normalized angular velocity auto-correlation function.
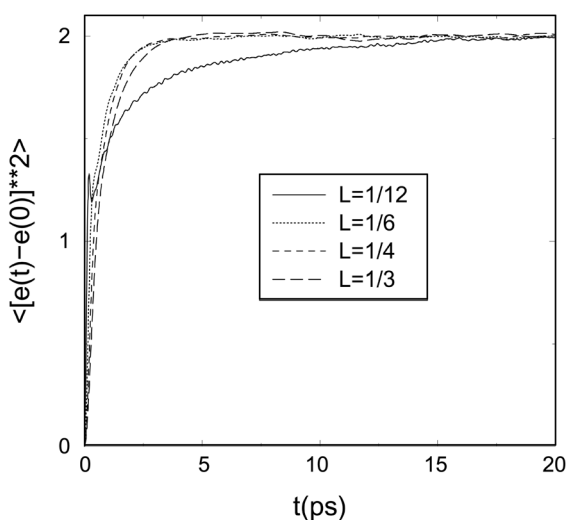

Figure 6. Mean square displacements of unit orientation vector.

the second term in the last equation goes zero as time goes infinity.

Rewriting Eq. (6) in terms of the normalized angular velocity auto-correlation function,

$$D_r = \frac{l^2}{2}\langle w^2 \rangle \int_0^\infty dt \frac{\langle w_i(0) \cdot w_i(t) \rangle}{\langle w_i(0) \cdot w_i(0) \rangle}, \qquad (25)$$

since the rotational temperature, $T_r = Iw^2/2$, is a constant and the inertia of momentum for diatomic molecule is given by $I = 2m(l/2)^2 = ml^2/2$, $l^2w^2/2 = 2T_r/m$ is a constant. The rotational diffusion coefficient depends on only the integral of the normalized angular velocity auto-correlation function in Figure 5. As the molecular elongation of diatomic molecules increases, random rotation decreases and the rotational diffusion coefficients for L= 1/4 and 1/3 are almost the same in the statistical error.

Shear viscosities by translational motions and shear spin viscosities by rotational motion calculated from our equilibrium MD simulations are list in Table 3. Translational viscosity of the spherical monatomic molecule at

Table 3. Shear (η_t, mp) and shear spin viscosities (η_r, 10^{-24} kg/ m·sec) of monatomic and diatomic molecules at 94.4 K obtained through the Green-Kubo and Einstein formulas. Uncertainties (standard deviations) in the last reported digit(s) are given in parenthesis.

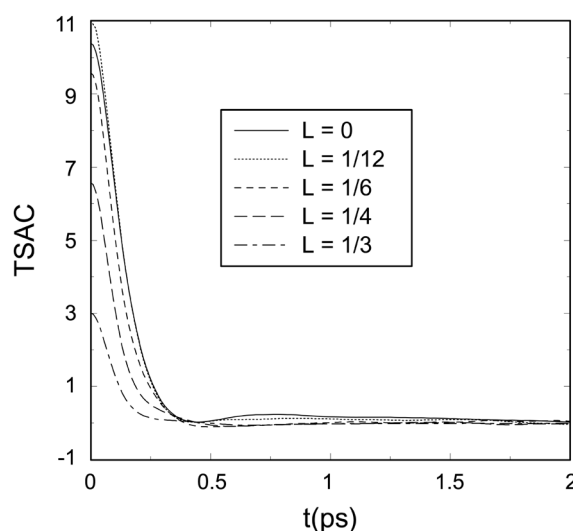|	L = 0	L = 1/12	L = 1/6	L = 1/4	L = 1/3
η_t, Eq. (9)	3.09(31)	26.6(23)	26.8(15)	24.0(13)	20.5(35)
η_t, Eq. (10)	3.08(1)	2.81(5)	2.05(3)	1.28(5)	0.62(6)
η_r, Eq. (11)	–	0.350(18)	1.86(9)	3.78(21)	6.03(40)
η_r, Eq. (12)	–	0.0034(8)	0.0431(6)	0.121(4)	0.148(2)

Figure 7. Translational stress [Eq. (10)] auto-correlation function.
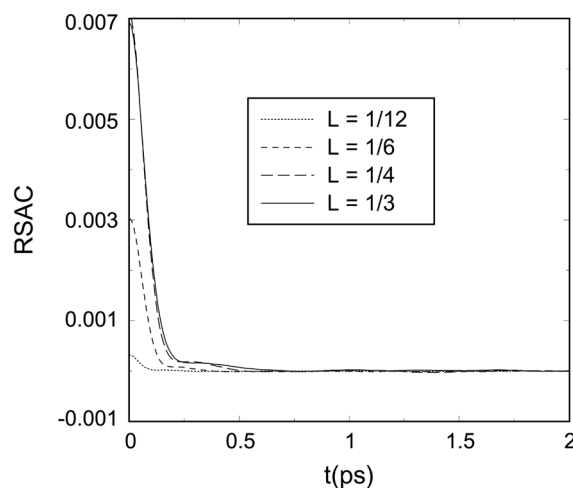

Figure 8. Rotational stress [Eq. (13)] auto-correlation function.

94.4 K shows a very close result with the experimental viscosity of liquid argon (1.97 mp[22]). Two shear viscosities obtained from different translational stresses, Eqs. (9) and Eq. (10), and two shear spin viscosities obtained from different translational stresses, Eqs. (12) and Eq. (13) for diatomic molecules show a difference in order of magnitude each other. Referring the shear viscosity of the spherical monatomic molecule, the first values of shear viscosity and

Table 4. Thermal conductivities (λ in 10^{-7} cal/K·cm·sec) of monatomic and diatomic molecules at 94.4 K obtained through the Green-Kubo. Uncertainties (standard deviations) in the last reported digit(s) are given in parenthesis. parenthesis.

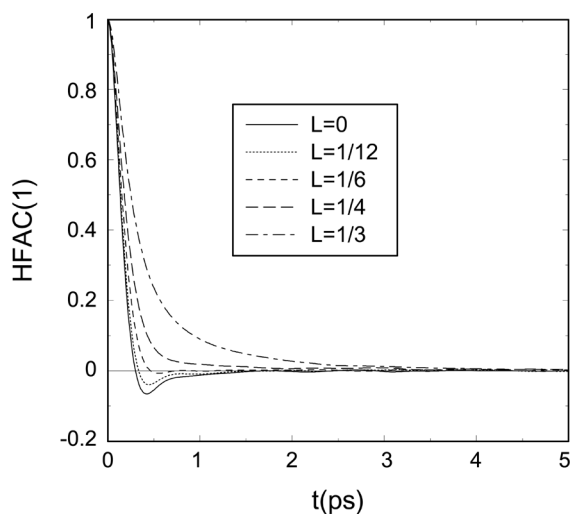|	L = 0	L = 1/12	L = 1/6	L = 1/4	L = 1/3
λ_{tt}, Eq. (18)	145(7)	166(2)	210(10)	276(7)	368(19)
λ_{tr}, Eq. (19)	–	42(4)	12(1)	16(2)	21(3)
λ_{tp}, Eq. (20)	791(51)	871(20)	828(39)	715(41)	463(60)
λ_{it}, Eq. (21)	773(16)	813(34)	741(23)	590(30)	346(53)
λ_{ir}, Eq. (22)	–	5.6(1)	53(1)	91(3)	109(11)
λ_{tot}, Eq. (23)	1709	1898	1844	1688	1307

Figure 9. Normalized heat flux ($\dot{q}_{ia}^{tt}$) auto-correlation function.

Figure 10. Normalized heat flux ($\dot{q}_{ia}^{tr}$) auto-correlation function.

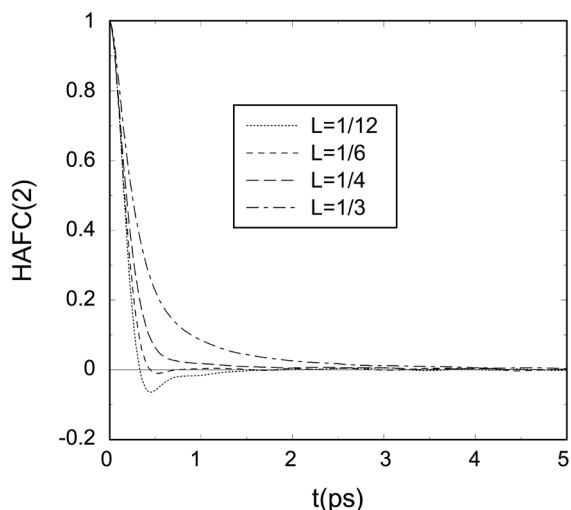**Figure 11**. Normalized heat flux ($\dot{q}_{ia}^{tp}$) auto-correlation function.
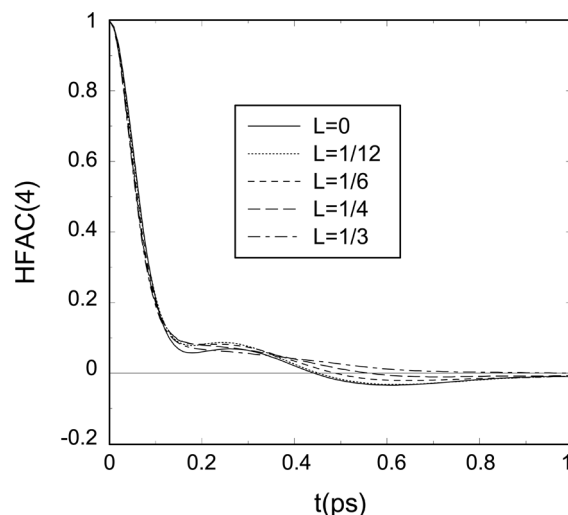
Figure 12. Normalized heat flux ($\dot{q}_{ia}^{it}$) auto-correlation function.

those of shear spin viscosity for diatomic molecules should be discarded.

Figures 7 and 8 shows the translational and rotational stresses, respectively. As the molecular elongation of diatomic molecule increases from the spherical monatomic molecule, the height of the translational stress auto-correlation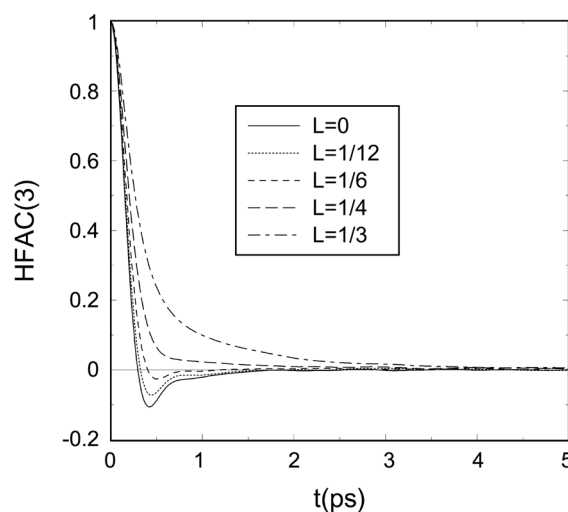 function decreases and accordingly the shear viscosity decreases, while for the shear spin viscosity the opposite is observed.

Energy transported *via* molecular motion governs heat conduction in gases, while energy transfer between molecules due to molecular interaction is a dominant factor in heat conduction in liquids. Liquid molecules transport energy by molecular motion and transfer their energy to other molecules by molecular interaction. Each contribution to the total thermal conductivity, Eq. (23), for the spherical monatomic and diatomic molecules are shown in Table 4. Thermal conductivity of the spherical monatomic molecule at 94.4 K shows a very close result with the experimental viscosity of liquid argon (2740×10^{-7} cal/Kcm·sec^{22}). Several normalized heat flux auto-correlation functions are shown in Figures 9-13. Each correlation function corresponds to heat flux of Eqs. (18)-(22). Since the modified Green-Kubo formula, Eq. (14), for thermal conductivity is rewritten as :

$$\lambda = \frac{V}{kT^2}\langle \dot{q}_{i\alpha}(0)^2\rangle \int_0^\infty dt \sum_i \frac{\langle \dot{q}_{i\alpha}(0)\dot{q}_{i\alpha}(t)\rangle}{\langle \dot{q}_{i\alpha}(0)\dot{q}_{i\alpha}(0)\rangle}, \qquad (26)$$
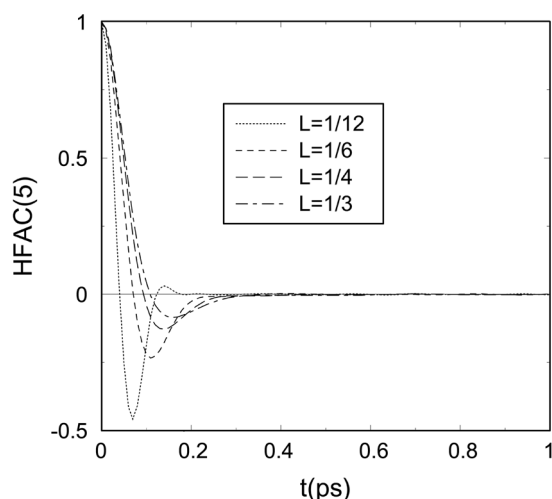
Figure 13. Normalized heat flux ($\dot{q}_{ia}^{ir}$) auto-correlation function.

is related to two facotrs - the average of square of heat flux at time 0 and the time integration of the normalized heat flux auto-correlation function.

The normalized heat flux auto-correlation functions of heat fluxes due to translational, rotational and potential energy transport show a very similar trend as seen in Figures 9, 10 and 11 because each heat flux of each molecule i contains the velocity term, v_i, in Eqs. (18), (19) and (20). Thermal conductivity due to translational energy transport monotonically increase as the molecular elongation of diatomic molecule increases from the spherical monatomic molecule, while for the thermal conductivities due to potential energy transport the opposite is observed since the potential energy decreases with the molecular elongation of diatomic molecule as shown in Figure 2. The contribution of rotational energy transport is relatively slight.

The normalized heat flux auto-correlation functions of heat fluxes caused by translational and rotational energy transfer, Figures 12 and 13, are different from those auto-correlation functions of heat fluxes due to energy transport. Thermal conductivity due to translational energy transfer monotonically decreases with the molecular elongation of diatomic molecule since the translational energy transfer by molecular interaction is related to the potential energy, while for the thermal conductivities due to rotational energy transfer the opposite is observed and the magnitudes are relatively small compared with other contributions for thermal conductivity.

The total thermal conductivity obtained our NpT ensemble EMD simulation increases as the molecular elongation of diatomic molecule decreases from the spherical monatomic molecule (Table 4). This result is inconsistent with the NEMD simulation result for two-center Lennard-Jones molecules.[11] Including two terms for thermal conductivity which are related to the rotational degree of freedom of diatomic molecule, the calculated thermal conductivity gives almost the same result to our previous EMD simulation study[23] in which the terms related to the rotational degree of freedom of diatomic molecule were missing.

Conclusion

Isothermal-isobaric(NpT) molecular dynamics simulations for diatomic molecule systems are carried out at 94.4 K. The diatomic molecules are modeled by equating its volume to monatomic molecule like argon and by increasing the distance between nuclei. As the molecular elongation of diatomic molecules increases from the spherical monatomic molecule, Lennard-Jones potential energy and the total energy decrease, the volume increases. The distribution of translational energy shows a typical Maxwell-Boltzmann, indicating the simulation systems are well-equilibrated. The distribution of rotational energy has the maximum at 0 energy, while the distribution of rotational speed shows a typical Maxwell-Boltzmann. Translation diffusion coefficients obtained from velocity auto-correlation functions (VAC) by Einstein relation are in good agreement with those obtained from mean square displacements (MSD) by Green-Kubo relation for the spherical monatomic and diatomic molecule systems. As the molecular elongation of diatomic molecules increases from the spherical monatomic molecule, the diffusion coefficient increases, indicating that longish shape molecules diffuse more than spherical molecules. Rotational diffusion coefficients of diatomic molecules are not obtained from mean square displacements of unit orientation vector for all cases due to non-linear behavior, and for the L = 1/12 case since angular velocity auto-correlation function does not decay to zero. As the molecular elongation of diatomic molecules increases, random rotation decreases and the rotational diffusion coefficients are almost the same in the statistical error. Translational viscosity of the spherical monatomic molecule at 94.4 K shows a very close result with the experimental viscosity of liquid argon. As the molecular elongation of diatomic molecules increases from the spherical monatomic molecule, translational viscosity decreases. Rotational viscosity is much less than translational viscosity, indicating the pressure on the wall is contributed by translation motion not by rotational motion. In general rotational viscosity increases as the molecular elongation of diatomic molecules increases. Thermal conductivity of the spherical monatomic molecule at 94.4 K shows a very close result with the experimental viscosity of liquid argon. As the molecular elongation of diatomic molecules increases from the spherical monatomic molecule, the total thermal conductivity by energy transport decreases even though the translational diffusion increases, the total thermal conductivity by energy transfer also decreases, and accordingly the total thermal conductivity increases. However, thermal conductivities by translational energy transport and by rotational energy transfer increase with the molecular elongation of diatomic molecule.

References

1. Harp, G. D.; Berne, B. J. *Phys. Rev.* **1970**, *A2*, 975.

2. Rahman, A.; Stilllnger, F. H. *J. Chem. Phys.* **1971**, *55*, 3336.

3. Streett, W. B.; Tildesley, D. J. *Proc. R. Soc. Lond.* **1976**, *A348*, 485.

4. Barojas, J.; Levcsque, D.; Quentrec, B. *Phys. Rev.* **1973**, *A7*, 1092.

5. Cheung, P. S. Y.; Powles, J. G. *Mol. Phys.* **1975**, *30*, 921.

6. Singer, K.; Taylor, A.; Singer, J. V. L. *Mol. Phys.* **1977**, *33*, 1757.

7. Lee, S. H.; Cummings, P. T. *Mol. Sim.* **2001**, *27*, 115.

8. Lee, S. H.; Cummings, P. T. *J. Chem. Phys.* **1996**, *105*, 2044.

9. Lee, S. H.; Cummings, P. T. *Mol. Sim.* **2001**, *27*, 139.

10. Tokumasu, T.; Ohara, T.; Kamijo, K. *J. Chem. Phys.* **2003**, *118*, 3677.

11. Fernandez, G. A.; Vrabec, J.; Hasse, H. *Mol. Sim.* **2005**, *31*, 787.

12. Allen, M. P.; Tildesley, D. J. *Computer Simulation of Liquids*; Oxford Univ. Press: Oxford, 1987; p 234.

13. Gear, C. W. *Numerical Initial Value Problems in Ordinary Differential Equations*; Englewood Cliffs: NJ, Prentice Hall, 1971.

14. Evans, D. J. *Mol. Phys.* **1977**, *34*, 317.

15. Evans, D. J.; Murad, S. *Mol. Phys.* **1977**, *34*, 327.

16. Allen, M. P.; Tildesley, D. J. *Computer Simulation of Liquids*; Oxford Univ. Press: Oxford, 1987; p 88.

17. Lee, S. H. *Bull. Kor. Chem. Soc.* **2007**, *28*, 1371.

18. Allen, M. P.; Tildesley, D. J. *Computer Simulation of Liquids*; Oxford Univ. Press: Oxford, 1987; p 48.

19. Evans, D. J.; Street, W. B. *Mol. Sim.* **1978**, *36*, 161.

20. Allen, M. P.; Tildesley, D. J. *Computer Simulation of Liquids*; Oxford Univ. Press: Oxford, 1987; p 64.

21. Lee, S. H.; Kim, H. S.; Pak, H. *J. Chem. Phys.* **1992**, *97*, 6933.

22. Cook, G. A. *Argon, Helium and the Rare Gases*; Intersciences: NY, 1961.

23. Lee, S. H. *Bull. Kor. Chem. Soc.* **2004**, *25*, 737.